

Nanoscale dynamics probed by laser-combined scanning tunneling microscopy

Hidemi Shigekawa^{*}, Shoji Yoshida, Osamu Takeuchi, Masahiro Aoyama, Yasuhiko Terada, Hiroyuki Kondo, Haruhiro Oigawa

Institute of Applied Physics, CREST-JST, 21st COE, University of Tsukuba, Tsukuba 305-8573, Japan

Available online 29 April 2007

Abstract

With the miniaturization of functional devices, the difference in the electronic properties, for example, due to the structural nonuniformity in each element of nanoscale blocks has an ever more crucial influence on macroscopic functions. Laser-combined scanning tunneling microscopy, a potential method that enables us to probe the photoinduced carrier dynamics on the nanoscale, is reviewed with the latest results.

© 2007 Elsevier B.V. All rights reserved.

Keywords: STM; Ultrashort-pulse laser; Pump-probe technique; Nanotechnology; Ultrafast phenomena

1. Introduction

“Smaller” and “faster” are the key concepts in nanoscale science and technology. Important and interesting phenomena in various systems, such as functional materials, electronic devices, signal transfer in biosystems, and chemical reactions, are observed from the several tens of nanometers to the single-molecule range in space and from the several tens of picoseconds to subpicosecond range in time. With the size reduction in structures, the difference in the electronic properties, for example, due to the structural nonuniformity in each element, has an ever more crucial influence on macroscopic functions. And the direct observation of the characteristics, which provides us with the basis for the macroscopic analysis of the results, is of great importance. Thus, for further advances, a method of exploring the transient dynamics of the local quantum functions in organized small structures is eagerly desired. However, it is difficult to obtain spatial and temporal resolutions simultaneously on this scale. Therefore, it is necessary to develop a new method, namely, new microscopy.

Scanning tunneling microscopy (STM) [1–4] has an excellent spatial resolution on the subangstrom scale and has fulfilled the needs of researchers in various fields. However,

since its temporal resolution is limited by the circuit bandwidth (~100 kHz), increasing its potential by, for example, combining its characteristics with those of other techniques has been desired. One of the promising approaches is to control the material conditions, in STM measurement, using the techniques of quantum optics. Ultrashort optical pulse technology in the near-infrared to ultraviolet region has enabled us to observe transient phenomena in the femtosecond range, the optical-monocycle region, which, however, has a drawback of a relatively low spatial resolution due to the electromagnetic wavelength. Therefore, since the invention of the STM almost 25 years ago, realizing the time-resolved tunneling current measurement in the subpicosecond range by developing STM combined with an ultrashort-pulse laser has been a challenging subject for obtaining the ultimate spatial and temporal resolutions simultaneously [5–23].

In this paper, we introduce our latest results obtained using the laser-combined STM and some related techniques.

2. Electronic structures probed on the nanoscale

In the world of nanofactories, as illustrated in Fig. 1, elemental blocks of various characteristics are integrated and organized on a designed stage to produce desired or new functions in a system on the macroscopic scale. However, to realize such a goal, the characterization and control of the

^{*} Corresponding author.

URL: <http://dora.ims.tsukuba.ac.jp/> (H. Shigekawa).

structures of each element are essential. Let us see the following examples.

Figs. 2a and b are an STM image of a Si nanoparticle of ~ 3 nm diameter on a graphite surface and the cross sections of the same region obtained at different sample bias voltages (+200 mV, +50 mV and -50 mV), respectively. Inhomogeneous structures are observed in the cross sections. Since STM provides information on the electronic structures at the observed bias voltage, the results indicate that there are complex electronic structures even at the single-molecule level (Fig. 2c). How can such a complex local dynamics work to produce a systematic function on the macroscopic scale?

In Fig. 3, contact atomic force microscopy (AFM) (a) and its tunneling current (b) images of quantum dots, formed on a GaAs/InP(113) surface, simultaneously obtained using a conductive cantilever are presented. A tunneling current of 0.2–0.5 nA was measured on quantum dots with a sample bias voltage of +0.2 V. In general, even though physical parameters are averaged, when observed using macroscopic techniques, inhomogeneous characteristic structures are observed; as shown in Fig. 3b. Since control of quantum dots is essential, for future optical technology, for example, detailed analysis of the electronic dynamics in each dot is extremely important.

Fig. 4 is a schematic illustration of the surface photovoltage (SPV). When the tip-sample distance is not sufficiently large and the scanning tunneling microscopy/spectroscopy (STM/STS) measurement is performed in the dark, tip induced band bending appears as illustrated in Fig. 4a, where a p-type semiconductor sample is used. When the sample below the STM tip is photoilluminated with a sufficient intensity, the introduction of photoexcited carriers reduces the band bending, resulting in the flat-band condition illustrated in Fig. 4b. This band bending change in the MIS structure is defined as an SPV, which is observed in STM measurement. Since the SPV is related to the local carrier dynamics induced by photoillumination [25–28], three-dimensional local electronic structures can be observed using this technique.

In Fig. 5, the bias-voltage-dependent SPV images of a Ag/Si(011) surface nanostructure are presented. The Ag islands formed on the Si(001) surface are marked using green lines in Fig. 5a. Fig. 5b to d are the mappings of the SPV measured at different bias voltages using light-modulated scanning tunneling spectroscopy (LM-STs) [23]. The variations in the SPV contour are caused by the change in the depletion layer due to

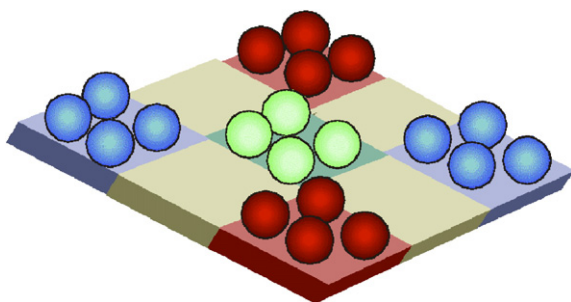


Fig. 1. Schematic illustration of nanoscale system.

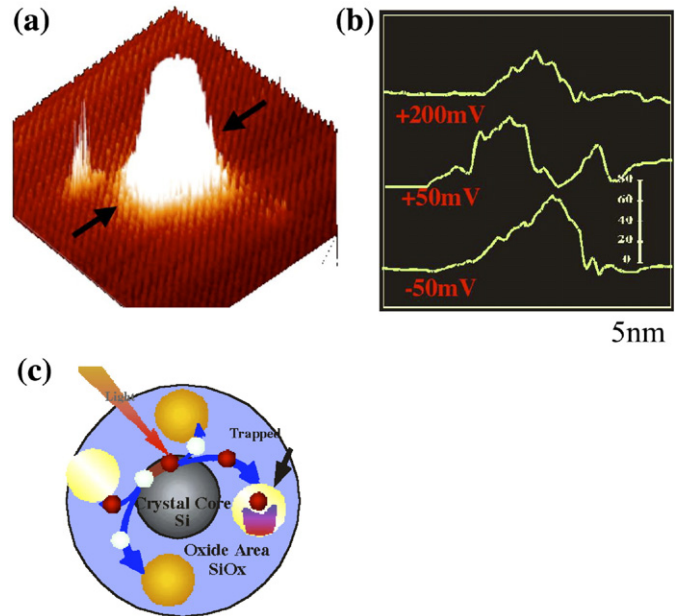


Fig. 2. STM image of Si nanoparticle (a) and cross section of the same region obtained at different bias voltages (b). (c) Diagram of the complex structures inside a nanoparticle.

tip-induced band bending, which is dependent on the applied bias voltage [24,28,29].

When this technique is applied to analyze a p–n junction under an operating condition, carrier flow, for example, depending on the forward bias voltage can be visualized through the measurement of the forward bias voltage-dependent SPV. Fig. 6 is an example obtained over a cleaved surface of a GaAs(110) p–n junction [28]. The change in the color of the left side, blue to red, shows the flow of holes injected from the p-type region for an increase in the forward bias voltage. The dynamics of the doped minor carriers plays an essential role in functional materials and devices. With the miniaturization of semiconductor devices, for example, the fluctuation in such electronic properties of each element has an ever more crucial influence on macroscopic functions. However, the electronic properties have been, in general, analyzed using the macroscopic behavior obtained from the data averaged over the operating area. These are the first results that provide a solid

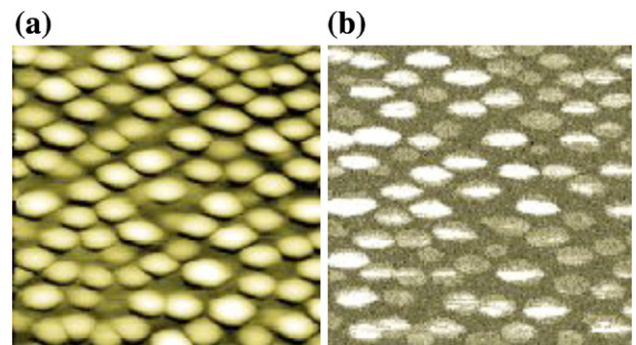


Fig. 3. Contact AFM (a) and tunneling current (b) images of quantum dots formed on GaAs/InP(113) surface.

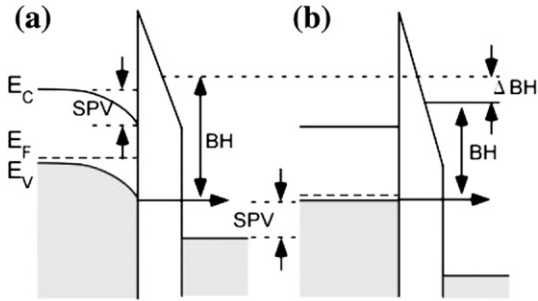


Fig. 4. Schematic illustrations of metal–insulator–semiconductor (MIS) structures in cases (a) without and (b) with photoillumination (BH: local barrier height).

basis for elucidating the mechanism of the carrier transport properties predicted by using the macroscopic analysis.

Can we obtain time-resolved information about the above-mentioned nanoscale dynamics using STM? In the next section, some examples of time-resolved measurements by STM are discussed.

3. Direct observation of dynamics by STM

In STM, a sharp tip is placed close to a target material, and information on the region underneath the STM tip is probed using a tunneling current (Fig. 7). In general, the STM is used as a probe under an equilibrium condition. However, when some perturbations, such as in temperature, electric field and photoillumination, are added from outside, we can analyze the dynamics of the system by observing responses to the change in the conditions.

Many works have been performed in this respect [2–4]. Fig. 8a is a schematic illustration of the structure of the azobenzene molecule. This molecule changes its conformation between

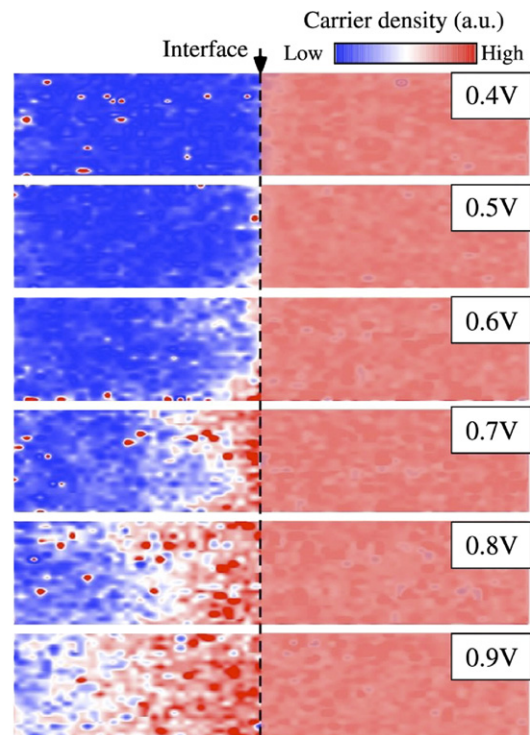
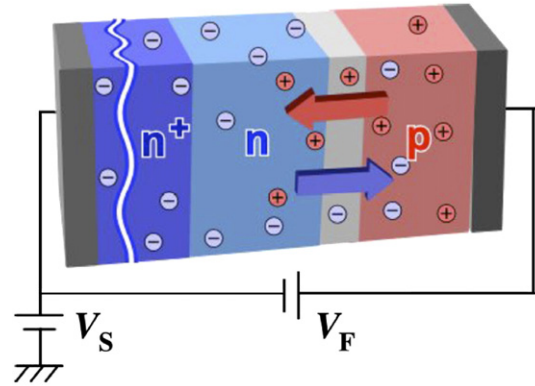


Fig. 6. Schematic illustration of a GaAs(100) pn junction and a series of carrier-flow mappings of injected holes at different forward bias voltages.

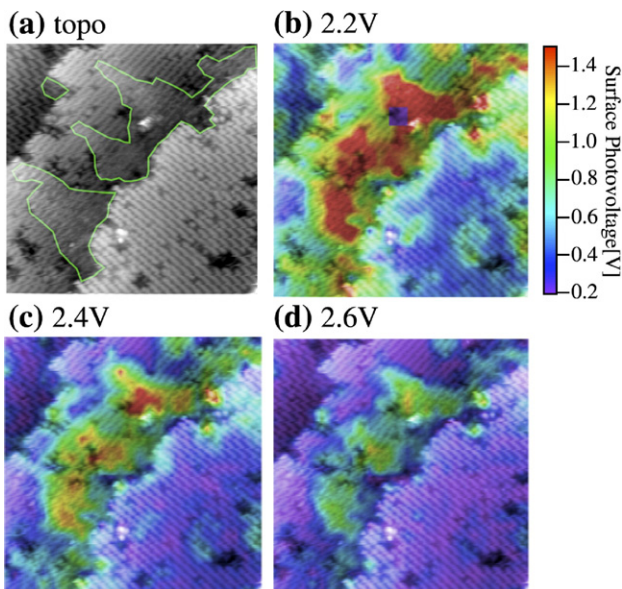


Fig. 5. Topographic STM (a) and bias-voltage-dependent surface photovoltage (SPV) images (b to d) obtained for Ag/Si(011) surface nanostructures (30 nm × 30 nm).

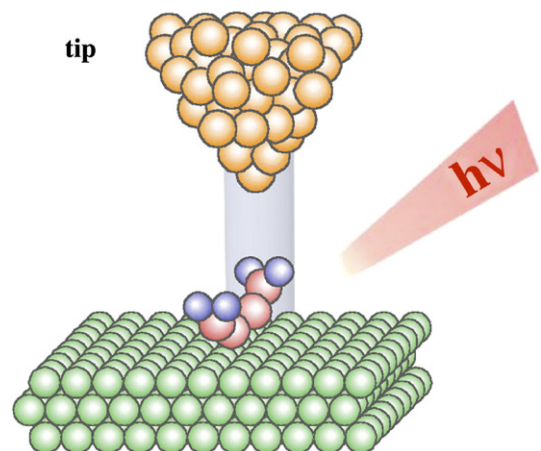


Fig. 7. STM setup with additional perturbation from outside (light in this case).

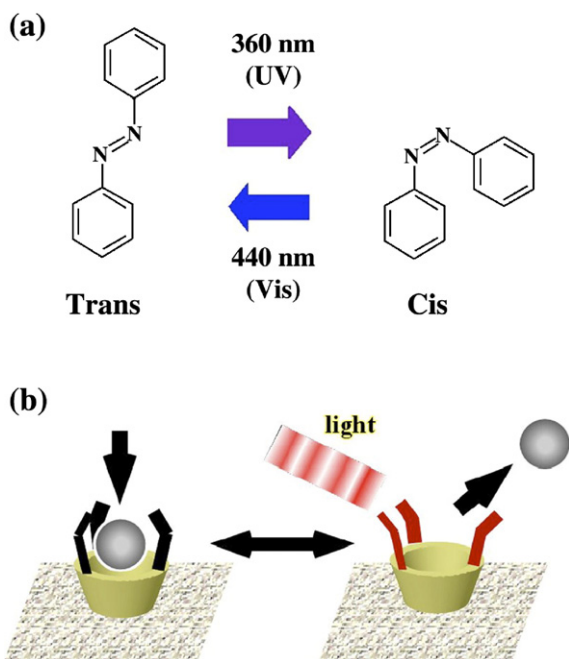


Fig. 8. (a) Schematic illustration of photoisomerization of azobenzene molecule. (b) Illustration of functional control using an azobenzene molecule.

trans and cis forms under visible (Vis, 440 nm) and ultraviolet (UV, 360 nm) lights. Thus, when functional molecules are modified using this molecule, new functions associated with switching mechanisms can be added to the original functions such as molecular recognition, sensing, and memory, as shown in Fig. 8b. Therefore, it is very important to analyze the structural change of the azo-molecule ([4-(phenyldiazenyl) phenyl]-*N*-(2-sulfanylethyl)carboxamide) at the single-molecule level [30–32].

Fig. 9a is an illustration of the STM setup [30]. The STM tip is placed just above an isolated azo-molecule embedded in a *n*-dodecanethiol (C_{12}) self-assembled monolayer (SAM) film formed on a Au(111) substrate. Samples were prepared by dipping gold-coated mica substrates into a solution with the target azo-molecule, and dodecanthiol molecules that were used as spacers to isolate azo-molecules. A photoinduced structural change was observed using STM under photoillumination as the wavelength was varied between Vis and UV wavelengths, alternately. Since an azo-molecule has a longer conformation in the trans form, it is supposed to be brighter under Vis light.

Fig. 9b is the result of the direct observation of the conformational change. The azo-molecule reversibly changes its image from bright to dark under Vis and UV lights, respectively, as expected. This change can be observed using STM at the single-molecule level. When we change the temperature, we can observe temperature-dependent phase transitions of materials at an atomic resolution [2–4,33–35]. However, it requires a long time to image such structural changes, for example, one minute for each image.

Without imaging, we can more rapidly observe structural changes. Fig. 10a is a schematic of such measurement. An STM tip is held just above a target, for example, a Si dimer on a Si(011) surface which rapidly flip-flops between two conforma-

tions even at 80K [36,37]. Since the tunneling current depends on the distance between the STM tip and the target material, structural changes can be determined from the corresponding change in the tunneling current. Fig. 10b shows the time dependence of the tunneling current measured by STM with the tip held just above a Si dimer. The tunneling current changes between two well-defined states, as expected. In this way, we can observe the dynamics of rapid structural changes. This method can be used to analyze the change in the dynamics of a single molecule [30,38,39]. However, as mentioned in the introduction, the maximum temporal resolution of STM is limited to ~ 100 kHz. Recently, chemical reaction and molecular motion induced by ultrashort laser pulses were successfully analyzed [40,41], but these measurements provide only a snapshot of the dynamics and still leave room for further advancement.

4. Laser-combined STM

4.1. Optical pump-probe technique

Let us see here briefly how fast another method, the optical pump-probe technique is [21,42]. When ultrashort laser pulses are produced at 80 MHz, the original pulse train is ~ 10 ns between two subsequent pulses, as highlighted in Fig. 11b. Each pulse is divided into two pulses with a delay time t_d (Fig. 11a), to form a train of pulse pairs as illustrated in Fig. 11c. We can control the delay time by changing the optical length of the delay time system shown in Fig. 11a.

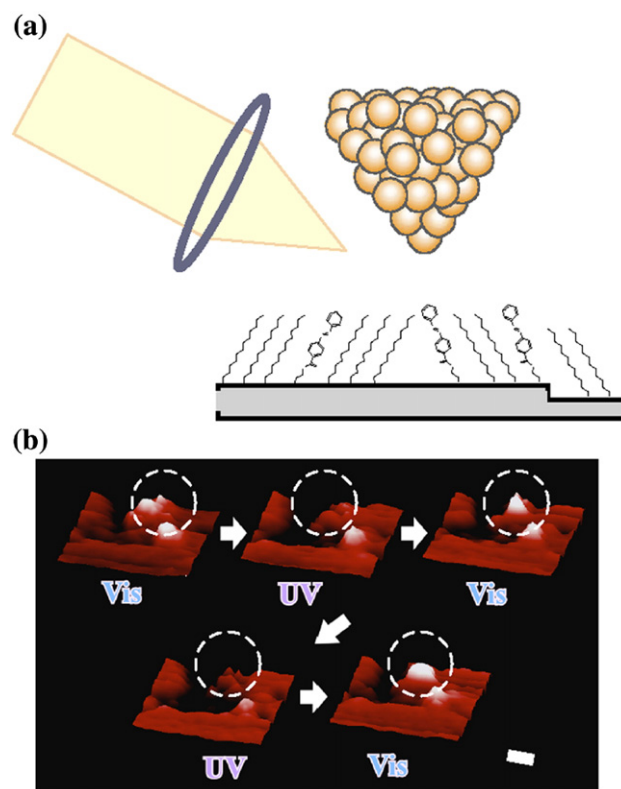


Fig. 9. (a) Schematic of STM measurement setup. (b) Photoisomerization of azobenzene molecule directly observed by STM. Vis and UV indicate visible and ultraviolet lights, respectively.

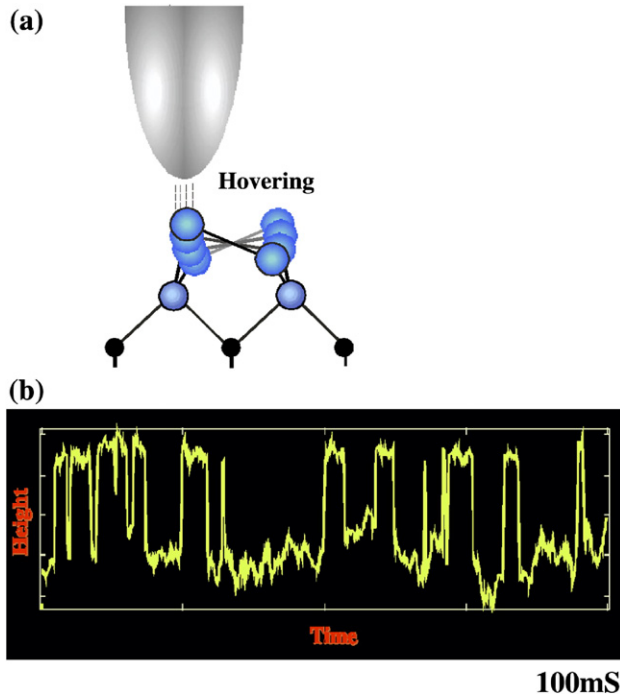


Fig. 10. Schematic of STM setup for observing flip-flop motion of Si dimer (a) and its result (b). Tunneling current changes between two well-defined states.

First pulses are used as a pump to excite the sample surface and second pulses are used as a probe to observe the relaxation of the excited state induced by the pump pulse, as shown in Fig. 12a. Since the reflectivity of the second pulses depends on the surface conditions, if the reflectivity of such pulses is measured as a function of the delay time, we can obtain information on the relaxation of the excited state through the change in reflectivity (Fig. 12b). In this case, the time resolution is limited only by the pulse width, in the ~ 1 fs range.

For comparison, spectra of the GaNAs sample obtained by the optical pump-probe technique is presented in Fig. 13 [17]. The reflectivity of the second pulses is plotted as a function of the delay time, which has two relaxation components of the

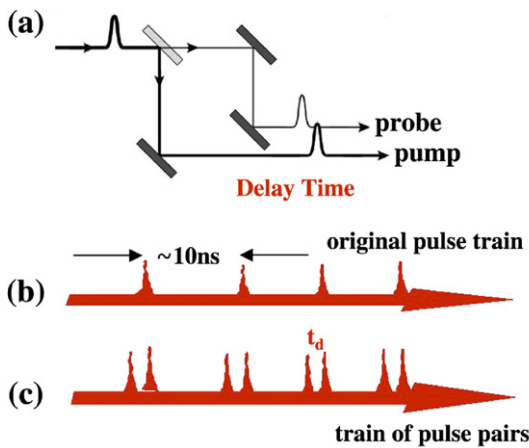


Fig. 11. (a) Schematic of optical delay time system. (b) Original laser pulse train oscillating at 80 MHz. (c) Train of laser pulse pairs (t_d : delay time).

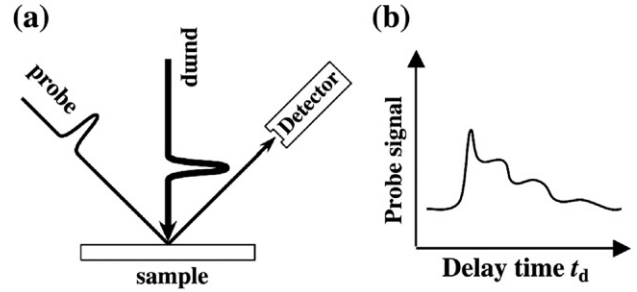


Fig. 12. Schematics of optical pump-probe measurement system (a) and obtained signal (b).

excited state ($\tau_{cool} = 5.3$ ps, and $\tau_{decay} = 400$ ps). These dynamics are attributed to the intra- and inter-band transitions of photocarriers [17,42–44].

4.2. Difficulties in combining STM with optical pump-probe technique

Now, one may want to combine the two techniques to achieve the ultimate resolutions in space and time simultaneously. However, there are many difficulties we have to overcome. Let us see two examples.

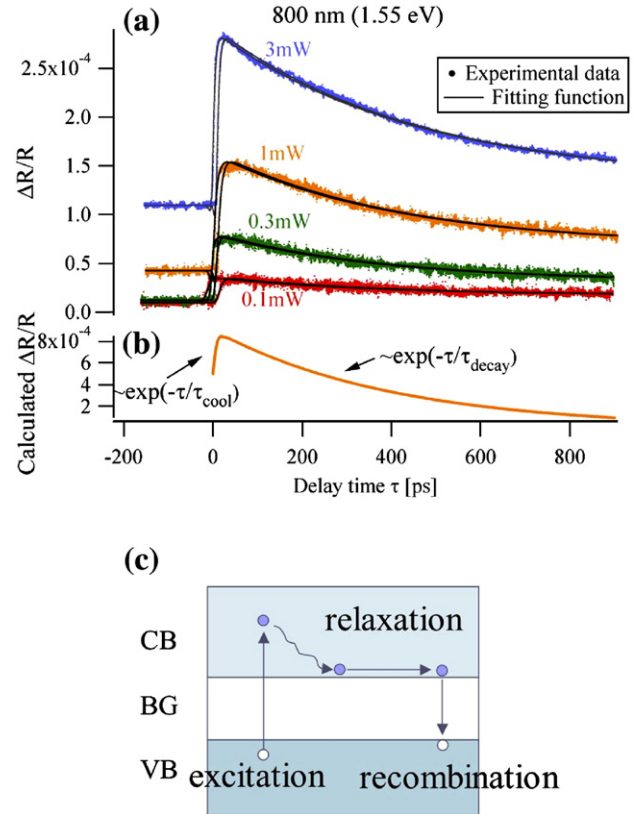


Fig. 13. (a) Result obtained by optical-pump-probe technique for GaN_xAs_{1-x} ($x=0.36\%$) sample. Excitation: 800 nm, pump (3 mW), probe (0.3 mW). (b) Fitting function. (c) Schematic of the excitation and relaxation process (CB: conduction band, BG: band gap, VB: valence band).

4.2.1. Temporal resolution of STM

As mentioned, the temporal resolution of STM is limited to ~100 kHz, worse than 10 μs. Therefore, although an ultrashort-pulse laser has now provided a temporal resolution of ~1 fs, we still cannot observe the dynamics of rapid changes, for example, in the picosecond range, by STM (Fig. 14). Since the development of STM, many researchers have pursued this goal [5–22] but have not yet succeeded; probing the dynamics of rapid changes based on a tunneling current is a critical point.

4.2.2. Thermal expansion of STM tip

Tunneling current depends exponentially on tip-sample distance, when the distance changes by 0.1 nm, tunneling current changes by one order. Fig. 15 shows the change in tunneling current as a function of time, representing the stability of the tunneling current. A tungsten tip and a Au(111) surface were used for the measurement. As Fig. 15a indicates, the signal obtained without photoillumination is very stable; however, when the tunnel gap is photoilluminated with chopped light, tunneling current is modulated at the same frequency due to the thermal expansion and shrinking of the STM tip and the sample surface, as indicated in Fig. 15b.

As will be discussed in the next section, we need to modulate the excitation to use a lock-in technique for measuring the weak target signal induced by ultrashort laser pulses. Since the change in tunneling current due to thermal expansion is large, the elimination of this thermal expansion effect is another critical

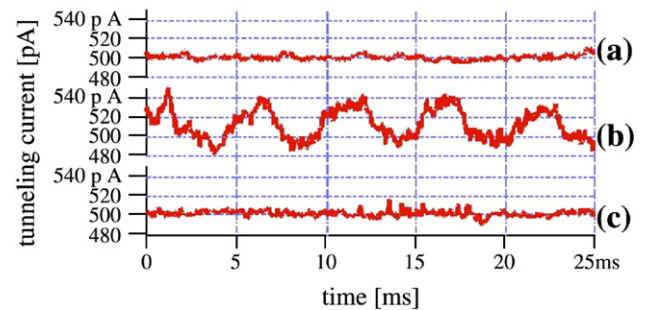
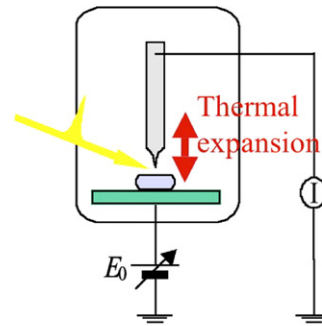
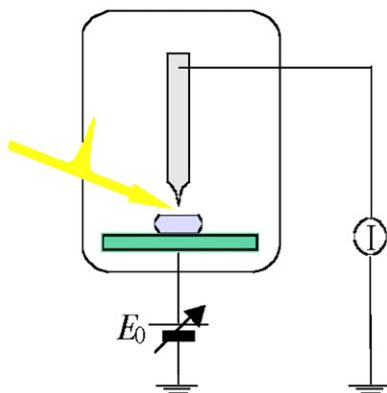


Fig. 15. Schematic of STM setup (upper) and the tunneling current as a function of time obtained (lower) (a) without photoillumination, (b) under chopped light, (c) by shaken pulse-pair-excited STM.

(a) STM + Laser excitation



(b)

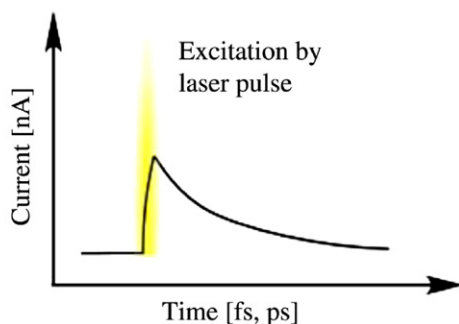


Fig. 14. (a) Schematic of the setup laser-combined STM and (b) A desired change in tunneling current excited by ultrashort-laser pulse.

problem that we have to overcome to combine STM with the ultrashort-pulse laser technique [13,22,45–47].

5. How to combine STM with optical pump-probe technique?

5.1. How to observe fast dynamics by STM?

Since the development of STM, many researchers have expended effort to observe fast dynamics by STM. The ultimate goal of this study is to analyze the electronic and structural dynamics of materials on the femtosecond scale at an atomic resolution.

There have been two major concepts proposed for achieving this goal. One is to introduce an ultrafast photoconductive gate into the current detection line of STM. This type of microscopy is called “photoconductively gated STM” [5]. Two laser beams consisting of a train of laser pulses are used to excite a sample and switch the photoconductive gate (Fig. 16). The photoconductive gate enables the sampling of instantaneous tunneling current induced on the sample by the excitation laser pulses. When the current is recorded as a function of the delay time between excitation and gating, the transient tunneling current is presumed to be reproduced on a real-time scale. However, the detected signal is primarily due not to the tunneling current but to the displacement current generated by the coupling of two stray capacitances; the first at the tunneling junction and the other at the photoconductive gate.

In another approach, a tunneling junction is excited by a sequence of laser pulses, and an induced tunneling current is

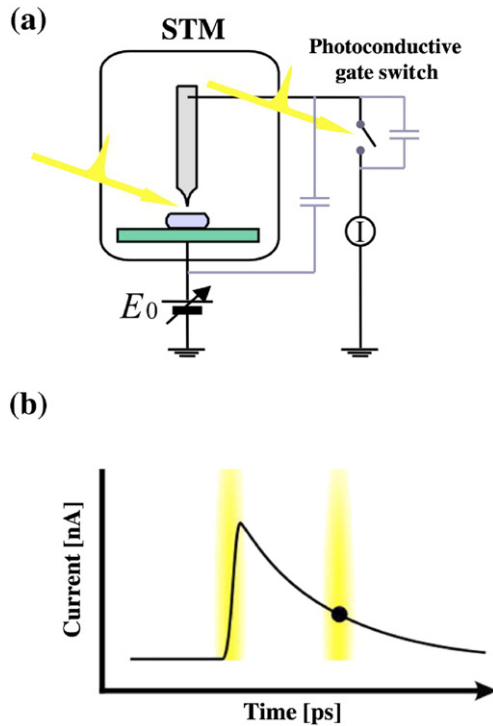


Fig. 16. Schematics of a photoconductively gated STM system (a) and its measurement scheme (b).

measured as a function of interpulse spacing (Fig. 17). As pioneering work, the carrier relaxation time at the Si(111)- 7×7 surface was determined with an approximately 10 ns time and a 1- μm spatial resolution [9]. The sample surface just under the STM tip was irradiated with a train of laser pulses because the surface potential is modulated by the irradiation due to the surface photovoltage effect. The displacement current can be probed using the STM tip when the irradiation is switched from on to off, and vice versa. Since displacement current depends on the change in band bending during the interpulse period of the laser pulses, the signal as a function of the repetition time of the laser pulses provides information on the band relaxation mechanism. This technique is applicable, but the spatial resolution is limited to $\sim 1 \mu\text{m}$, since the signal is a displacement current. Moreover, since the repetition rate of laser pulses is

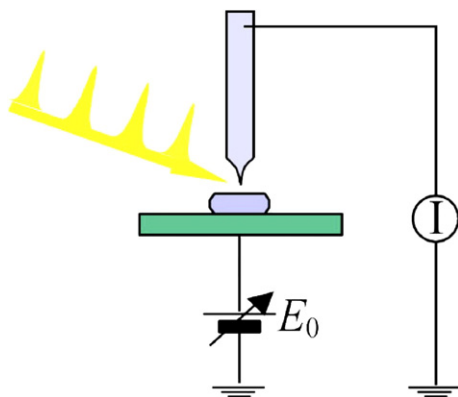


Fig. 17. Schematic of pulse-laser-excited STM.

changed by thinning out the laser pulses from the original pulse train, the time resolution is limited by the repetition rate of the original pulse train, $\sim 100 \text{ MHz}$ (10 ns).

To obtain a time resolution higher than the repetition rate, a new method, called “pulse-pair-excited STM” was proposed [6–22]. The measurement of the tunneling current using STM ensures an atomic resolution.

5.2. Pulse-pair-excited STM

For the conventional optical pump-probe technique, as shown in Fig. 12a, the electronic structures of a target material are excited using the pump laser pulses and then relax over time. The reflectivity of the second laser pulses is measured as a function of the delay time. Thus, the change in reflectivity with the delay time is analyzed as a signal associated to the relaxation of the excited state (Fig. 12b).

For a laser-combined STM, the sample surface under the STM tip is modulated with two laser pulses, and the change in the tunneling current depending on the delay time is analyzed. One is called junction-mixing STM (JM-STM), in which the tunneling impedance is electrically modulated with a combination of photoconductive switches and laser pulse pairs; thus, the tunneling current produces a change due to the inherent nonlinearity of the current-voltage characteristic [6–14]. In another approach, the surface under the STM tip is photo-illuminated with the paired pulses (Fig. 18). Then the change in the optical pump-probe signal or the average tunneling current instead of the reflectivity of the second pulses is measured as a function of the delay time t_d . The former (JM-STM) is similar to the conventional optical pump-probe technique and the effect of the STM tip gives us the local information [15], while the latter provide us with the time-resolved tunneling current with the STM spatial resolution.

Let us determine the probe for a pulse-pair-excited STM. In Fig. 19 the relationship between the tunneling current induced by a pair of laser pulses and the delay time of the two pulses are presented. When the delay time is long, change in the tunneling current induced by the two laser pulses contributes to the average tunneling current independently, and their amounts are the same. For a delay time shorter than the relaxation time of the excited state induced by the first pulse, and for the nonlinear

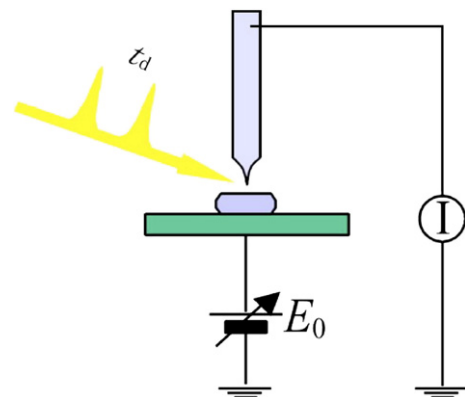


Fig. 18. Schematic of pulse-pair-excited STM.

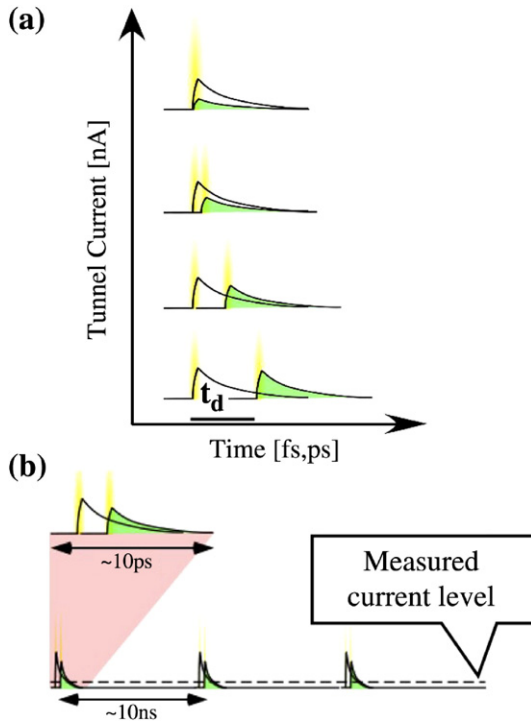


Fig. 19. Relationship between tunneling current induced by paired laser pulses and delay time of the two pulses.

interference between excitations by the two pulses, the tunneling current induced by the second pulses depends on the delay time. In such a case, the average current also changes as a function of the delay time. Thus, the dynamics of the electronic structure of a target material can be probed using the tunneling current, at the pulse width resolution, that is, in the femtosecond range.

5.3. How to treat thermal expansion?

Since the signal is weak, we need to use a lock-in detection measurement method. In such a case, excitation is modulated at a frequency and the corresponding change in tunneling current is measured as a signal. However, as mentioned in Section 4.2.2, intensity modulation (Fig. 20a) strongly influences the stability of the tunneling current (Fig. 15b). A promising way is to modulate the delay time instead of intensity (Fig. 20b), in which the modulation frequency can be chosen independently of any noises. Fig. 15c is the stability of the tunneling current measured using this method under photoillumination. To evaluate the thermal expansion effect caused by photoillumination, a Au surface was used as a sample in which a negligible photoinduced signal is expected. In fact, no thermal expansion effect in Fig. 15b is observable in this case, indicating that the weak target signal can be measured using this method.

6. Shaken pulse-pair-excited STM (SPPX-STM)

Here, new microscopy using the method described in 5.3 is explained in more detail [17–22]. Fig. 21 is a schematic of

the femtosecond time-resolved STM that we developed. Each laser pulse is divided into two pulses to form a train of pair pulses. The sample just under the STM tip is photoilluminated and the average tunneling current is measured as a function of delay time. Since the lock-in method is used to measure a weak signal with the modulation of delay time, the first signal obtained is differentiated tunneling current (dI/dt_d), which is a function of delay time. Therefore, after the numerical integration of the signal, a spectrum could be obtained that was compared with the conventional optical pump-probe technique shown in Fig. 13a.

Fig. 22 is the result obtained from the SPPX-STM for a GaNAs sample. The differentiated spectrum of the dashed line is obtained first as a signal. Using the numerical integration of the signal, the tunneling current deviation can be estimated from the solid line, which can be compared with the result of Fig. 13a.

As shown in Fig. 22, tunneling current changes in the picosecond range; however, the shape of the spectrum may differ from that obtained using the optical pump-probe technique. Because the probe is tunneling current in this case, the signal appears even in the negative-delay-time region. Fig. 22 also shows the fitting function (dashed-dotted line) consisting of the sum of two exponential functions and a constant, $\sum_i A_i \exp(-\tau/\tau_i^{STM}) + \text{const} (i = 1, 2)$, that gives the best fit to the ΔI curve. The ΔI curve consists of two decay components that reflect ultrafast phenomena induced by laser illumination. The faster component ($\tau_1^{STM} = 118$ ps) has a positive amplitude ($A_1 > 0$), while the slower one ($\tau_2^{STM} = 550$ ps) has a negative amplitude ($A_2 < 0$).

Roughly speaking, there are two different types of nonlinearity: (i) divergent and (ii) saturation prone [17]. The divergent and saturation-prone nonlinearities are expressed here as $I_t(t) \propto n(t)^k (k > 1)$ and $I_t(t) \propto n(t)^k (k < 1)$, respectively; where I_t is the transient tunneling current and n is the photocarrier density. Under the assumption of exponential decay of carrier density, $n(t) \sim \exp(-t/\tau_{\text{decay}})$, the divergent nonlinearity is characterized by a maximum in ΔI at $\pi = 0$ where a decrease is observed when π is increased, whereas

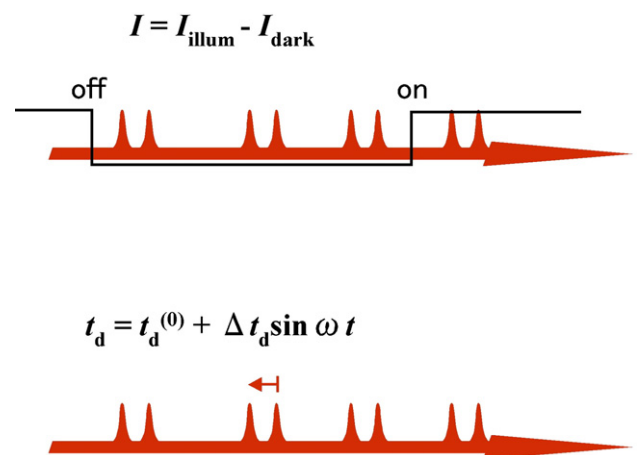


Fig. 20. (a) Intensity and (b) delay-time modulations of light for lock-in detection.

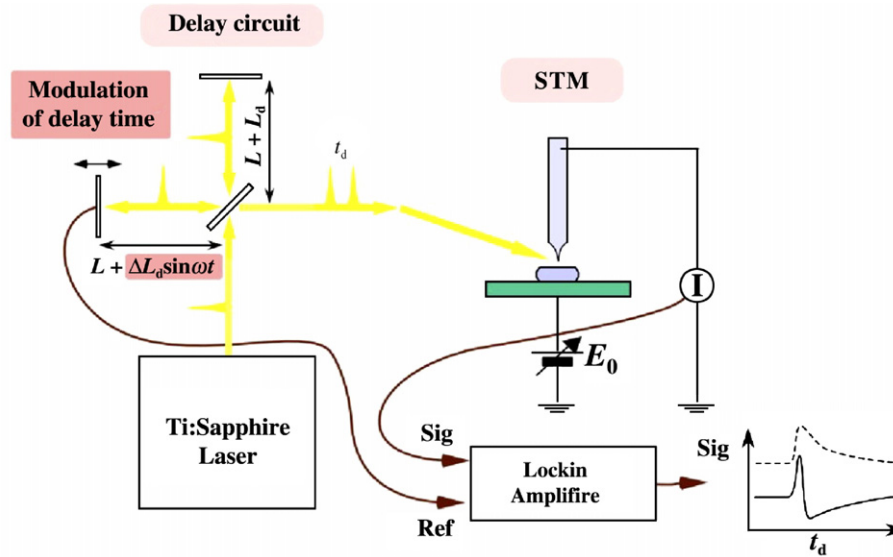


Fig. 21. Schematic of shaken pulse-pair-excited STM system.

the saturation-prone nonlinearity is characterized by a minimum in ΔI at $\pi=0$ and ΔI increases when π is increased. From the characteristics of the delay-time dependence of the signals, the slower one can be attributed, for example, to the process of photocarrier recombination, which is in good agreement with that obtained using the optical pump-probe technique (Fig. 13) [17].

To confirm that what observed is a tunneling current, the change in signal intensity was measured as a function of total tunneling current by changing the distance between the tip and the sample. As in Fig. 23, there is a clear linear relationship between these parameters, indicating that the signal is a tunneling current and not another signal such as photoemission [18]. Since the tunneling current is measured as the probe in this method, rapid dynamics can be observed at the STM resolution.

Recently, we have succeeded in developing a new version where the S/N ratio is 100 times better than that of the present technique. With this method, we are now conducting the

direct mapping of photo carrier dynamics in various materials on the nanoscale; details of which will be published elsewhere.

7. Conclusion

We have reviewed the basis of laser-combined STM, especially the femtosecond time-resolved STM that enables us to observe the dynamics of electronic structures with the ultimate spatial and temporal resolutions. This new technique is expected to contribute to advance future research in nanoscale science and technology, in terms of the ultimate temporal and spatial resolutions.

The work about SPPX-STM was supported in part by a Grant-in-Aid for Scientific research from the Ministry of Education, Culture, Sports, Science, and Technology of Japan. We thank Ms. Rie Yamashita in our group at University of Tsukuba for her help in preparing this paper.

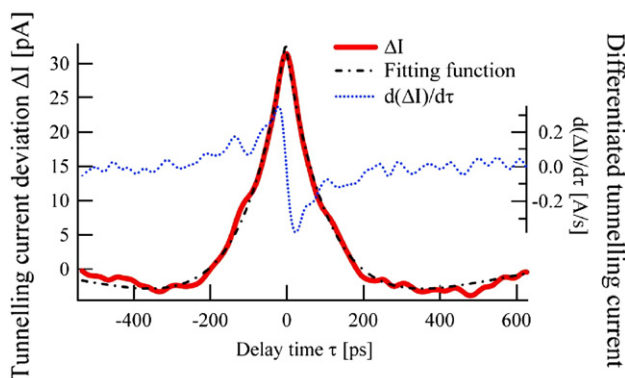


Fig. 22. Result obtained by SPPX for $\text{GaN}_x\text{As}_{1-x}$ ($x=0.36\%$) sample.

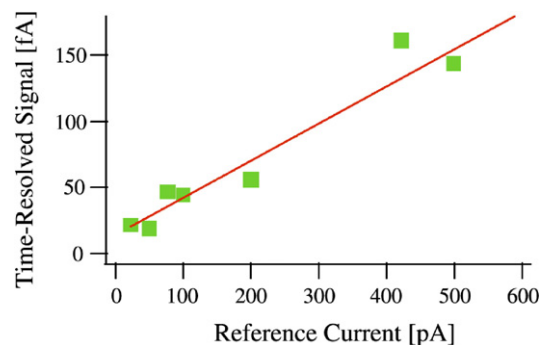


Fig. 23. Relationship between time-resolved signal intensity and average tunneling current, measured while varying tip-sample distance.

References

- [1] G. Binnig, H. Rohrer, Dh. Gerber, E. Weibel, *Phys. Rev. Lett.* 50 (1983) 120.
- [2] T. Sakurai, Y. Watanabe (Eds.), *Advances in Scanning Probe Microscopy*, Springer, 2000.
- [3] R. Wisendanger (Ed.), *Scanning Probe Microscopy*, Springer, 1998.
- [4] *Applied Scanning Probe I. Methods, II, III, IV*, in: B. Bhushan, H. Fuchs (Eds.), Springer, 2000, 2004.
- [5] S. Weiss, D. Botkin, D.F. Ogletree, M. Salmeron, D.S. Chemla, *Phys. Status Solidi, B Basic Res.* 188 (1995) 343.
- [6] M.R. Freeman, A.Y. Elezzabi, G.M. Steeves, G. Nunes Jr., *Surf. Sci.* 386 (1997) 290.
- [7] R.H.M. Groeneveld, H. van Kempman, *Appl. Phys. Lett.* 69 (1996) 2294.
- [8] N.N. Khusnatdinov, T.J. Nagle, G. Nunes Jr., *Appl. Phys. Lett.* 77 (2000) 4434.
- [9] R.J. Hamers, D.G. Cahill, *J. Vac. Sci. Technol.*, B 9 (1991) 514.
- [10] S. Grafstrom, *J. Appl. Phys.* 91 (2002) 1717.
- [11] D.A. Yarotski, A.J. Taylor, *Appl. Phys. Lett.* 81 (2002) 1143.
- [12] W. Pfeiffer, F. Sattler, S. Vogler, G. Gerber, J. Gr. R. Moller, *Appl. Phys., B Lasers Opt.* 64 (1997) 265.
- [13] V. Gerstner, A. Knoll, W. Pfeiffer, A. Thon, G. Gerber, *J. Appl. Phys.* 88 (2000) 4851.
- [14] A. Thon, M. Merschforf, W. Pfeiffer, T. Klamroth, P. saalfrank, D. Diesing, *Appl. Phys., A* 78 (2004) 189.
- [15] M. Feldstein, P. VVohringer, W. Wang, N. Scherer, *J. Phys. Chem.* 100 (1996) 4739.
- [16] T. Brixner, F. Garcia de Abajo, J. Schneider, W. Pfeiffer, *Phys. Rev. Lett.* 95 (2005) 093901.
- [17] Y. Terada, M. Aoyama, H. Kondo, A. Taninaka, O. Takeuchi, H. Shigekawa, *Nanotechnology* 18 (2007) 044028.
- [18] O. Takeuchi, M. Aoyama, R. Oshima, Y. Okada, H. Oigawa, N. Sano, R. Morita, M. Yamashita, H. Shigekawa, *Appl. Phys. Lett.* 85 (2004) 3268.
- [19] O. Takeuchi, M. Aoyama, H. Kondo, Y. Terada, H. Shigekawa, *Jpn. J. Appl. Phys.* 45 (2006) 1956.
- [20] O. Takeuchi, M. Aoyama, H. Shigekawa, *Jpn. J. Appl. Phys.* 44, 7B (2005) 5354.
- [21] M. Yamashita, H. Shigekawa, R. Morita (Eds.), *Mono-cycle Photonics and Optical Scanning Tunneling Microscopy*, Springer Series in Optical Sciences, 2005.
- [22] H. Shigekawa, O. Takeuchi, M. Aoyama, *Sci. Technol. Adv. Mater.* 6 (2005) 582.
- [23] O. Takeuchi, S. Yoshida, H. Shigekawa, *Appl. Phys. Lett.* 84 (2004) 3645.
- [24] S. Yoshida, J. Kikuchi, Y. Kanitani, O. Takeuchi, H. Oigawa, H. Shigekawa, *e-J. Surf. Sci. Nanotechnol.* 4 (2006) 192.
- [25] R.J. Hamers, K. Markert, *J. Vac. Sci. Technol.* A8 (4) (1990) 3524.
- [26] L. Kronik, Y. Shapira, *Surf. Sci. Rep.* 37 (1999) 1.
- [27] S. Aloni, I. Nevo, G. Hasse, *J. Chem. Phys.* 115 (2001) 1875.
- [28] S. Yoshida, Y. Kanitani, R. Oshima, O. Takeuchi, Y. Okada, H. Shigekawa, *Phys. Rev. Lett.* 98 (2007) 026802.
- [29] M. Weimer, J. Kramar, J.D. Baldeschwieler, *Phys. Rev.*, B 39 (1989) 5572.
- [30] S. Yasuda, T. Nakamura, M. Matsumoto, H. Shigekawa, *J. Am. Chem. Soc.* 125 (2003) 16430.
- [31] T. Hugel, N. Holland, A. Cattani, L. Moroder, M. Seitz, H. Gaub, *Science* 296 (2002) 1103.
- [32] B. Choi, S. Kahng, S. Kim, H. Kim, H. Kim, Y. Song, J. Ihm, Y. Kuk, *Phys. Rev. Lett.* 96 (2006) 156106.
- [33] S. Yoshida, T. Kimura, O. Takeuchi, K. Hata, H. Oigawa, T. Nagamura, H. Shigekawa, *Phys. Rev.*, B 70 (2004) 235411.
- [34] H. Shigekawa, K. Hata, K. Miyake, M. Ishida, S. Ozawa, *Phys. Rev.*, B 55 (1997) 15448.
- [35] K. Hata, M. Ishida, K. Miyake, H. Shigekawa, *Appl. Phys. Lett.* 73 (1998) 40.
- [36] K. Hata, Y. Sainoo, H. Shigekawa, *Phys. Rev. Lett.* 86 (2001) 3084.
- [37] Y. Pennec, M. Hoegen, X. Zhu, D. Forthim, M. Freeman, *Phys. Rev. Lett.* 96 (2006) 026102.
- [38] T. Komeda, Y. Kim, M. Kawai, *Science* 295 (2003) 2055.
- [39] Y. Saino, Y. Kim, T. Okawa, T. Komeda, H. Shigekawa, M. Kawai, *Phys. Rev. Lett.* 95 (2005) 246102.
- [40] M. Durr, A. Biedermann, Z. Hu, U. Hofer, T. Heinz, *Science* 296 (2002) 1938.
- [41] L. Bartels, F. Wang, D. Moller, E. Knosel, T. Heinz, *Science* 305 (2004) 648.
- [42] J. Shah, *Ultrafast Spectroscopy of Semiconductors and Semiconductor Nanostructures*, Solid State Science Series, Springer, 1999.
- [43] Y. Lee, A. Chavez-Pirson, S. Koch, H. Gibb, S. Park, J. Morhange, A. Jeffery, M. Peyghambarian, L. Banyai, A. Gossard, W. Wiegmann, *Phys. Rev. Lett.* 57 (1986) 2446.
- [44] S. Prabhu, A. Vengurlekar, *J. Appl. Phys.* 95 (2004) 7803.
- [45] M. Nabil, S. Andrew, D. Ripple, *Appl. Phys. Lett.* 49 (1986) 137.
- [46] A. Bragas, S. Landi, J. Coy, O. Martinez, *J. Appl. Phys.* 82 (1997) 4153.
- [47] S. Grafstrom, P. Schuller, J. Kowalski, R. Neumann, *J. Appl. Phys.* 83 (1998) 3453.